NUMERICAL ANALYSIS OF FORCED CONVECTION HEAT TRANSFER FROM TWO TANDEM CIRCULAR CYLINDERS EMBEDDED IN A POROUS MEDIUM

by

Habib-Ollah SAYEHVAND [a*], ***Ehsan KHALILI DEHKORDI*** [a], **and *Amir BASIRI PARSA*** [b]

[a] Department of Mechanical Engineering, Bu-Ali Sina University, Hamedan, Iran
[b] Hamedan Branch, Islamic Azad University, Hamedan, Iran

Original scientific paper
https://doi.org/10.2298/TSCI150307081S

Study the heat and mass transfer in packed bed heat exchangers particularly in nuclear application is subject of many new researches. In this paper numerical analysis of forced convection heat transfer from two tandem circular cylinders embedded in a packed bed, which is made of spherical aluminum particles, is investigated in laminar flow. The porous medium increases the overall heat absorbed from two cylinders and cooling effect but increases the pressure drop, significantly. Also, the effect of increase the horizontal distance between two tandem circular cylinders on flow pattern and heat transfer is investigated. For the empty channel, the total wall heat flux in very small distances have a minimum due to generation of closed vortex region and for longer distances, by increases the distance between two tandem cylinder, the total wall heat flux increases. It is shown that for two circular cylinders embedded in the packed bed, the total wall heat fluxes from two cylinders and the fluid outlet temperature increase to a maximum quantity and then decrease with negative gradient. Also, the quantities of the empty channel are too smaller than the amounts of porous medium.

Key words*: porous medium, packed bed, forced convection, laminar flow, two tandem cylinders*

Introduction

Fundamental and applied research in flow, heat, and mass transfer in porous media has received increased attention during recent decades. A complete review on heat and mass transfer in porous media was performed by Goldstein *et al*. [1]. Vafai [2] reported the application of porous media in biotechnology and other modern industries. The application of packed beds with regular and irregular packing, changes the heat and mass transfer through the heat exchangers. There are lots of parameters, which governs the heat and mass transfer in packed bed, and should be investigated. Some of them were studied in [3-5] the same as wall effects, bed performance, temperature profiles in the bed, packing morphology, and flow rates in different flow regimes. Kaviany [6] stated that in packed beds in low Reynolds numbers, the Darcy law can be applied and it was unable to describe the flows at high Reynolds number. Therefore, many researches focused on the non-Darcian effects. Mahgoub [7] examined the non-Darcian forced convection heat transfer over a horizontal plate in a porous medium made by spherical particles. To consider inertia-effects, Hellstrom and Lundstrom [8] showed that the use of the

[*]Corresponding author, e-mail: hsayeh@basu.ac.ir

empirically derived Ergun equation, which can describe the response of several porous media, does not reveal the real mechanisms for some flows. Results of considerable experimental researches, on unconsolidated porous media, are gathered by Vafai [9]. Yuki *et al.* [10] preformed particle image velocimetry to identify the flow structures in a sphere-packed pipe. Also, Orodu *et al.* [11] used a simple experimental set-up to validate capillary tube models of flow in porous media.

Numerical simulations of heat and mass transfer in porous media have been developed increasingly.Verma and Mewes [12] carried out the three 3-D simulation of flow in packed bed of porous adsorbents using lattice Boltzmann methods. Yih-Ferng Peng *et al.* [13] used a nested-block finite volume based Cartesian grid method to simulate the unsteady viscous incompressible flows. Zdravkovich [14, 15] studied the characteristic of flow over cylinder and the complicated behavior of the interference in different arrangement of cylinders. Tatsuno *et al.* [16] experimentally studied the statistically stable posture of a triangular or a square cylinder and indicated that both cylinders come to rest in a stable posture with a side perpendicular to the uniform flow.

Flow over a cylinder embedded in porous medium is considered to increase the convection heat transfer mainly. The problem of cooling a pipe in heat exchangers using porous medium considered in many works. In many reactors, particularly nuclear reactors, increasing the cooling rate and heat transfer from a circular cylinder which is embedded in sands is a critical problem. One of the effective ways of increase the convection heat transfer is the use of porous medium instead of a single medium. Al-Sumaily *et al.* [17], numerically studies the time dependent forced convection heat transfer from a single circular cylinder embedded in a horizontal packed bed of spherical particles under local thermal non-equilibrium condition, using the spectral-element method. In another work Al-Sumaily *et al.* [18] studied the effect of porous media particle size on forced convection from a circular cylinder without assuming local thermal equilibrium between phases.

It is observed that when two cylinders horizontally or in tandem arrangement are located near each other, the regimes of heat and mass transfer is different from one cylinder, considerably. Kostic and Oka [19] carried out experimental investigations of the flow and heat transfer around two cylinders. They showed that for two cylinders in small distance, the closed vortex region or free cavity causes that the 2nd cylinder influenced on the 1st cylinder due to vortex, significantly and leads to a local minimum in heat transfer. Dehkordi *et al.* [20], investigated the 2-D unsteady viscous flow around two circular cylinders in a tandem arrangement in order to study the characteristics of the flow in both laminar and turbulent regimes. Koda and Lien [21], considered the aerodynamic effects due to the development of 3-D flow structures in the flow over one and two cylinders in tandem using the lattice Boltzmann method. Shyam and Chhabra [22], studied forced convection heat transfer from two square cylinders in tandem arrangement to power-law and Newtonian fluids.

As the literature review indicates the flow over two tandem circular cylinders in packed beds are not investigated completely and this problem should studied with more attention. In the present work, flow regime of two horizontally tandem circular cylinders embedded in packed bed is mentioned and numerically solved. First the flow regimes in empty and porous channel are compared. Then the streamlines, pressure gradient, forced convection heat transfer and outlet temperature is derived. Also, the main objective is to discuss the effect of the distance between two cylinders on overall heat transfer.

Problem description

Figure 1 indicates schematic of the problem. Laminar flow at low Reynolds number passes over two tandem circular cylinders immersed in a horizontal packed bed of spherical particles. The fluid is assumed to be Newtonian and incompressible. The cylinders are isothermally heated at a constant temperature, T_h, and they are cooled by the external fluid with U_0, T_0. The confining horizontal walls have the same temperatures $T_w = T_0$. The blockage ratio of the bed is $D_{cy}/H = 0.2$, where D_{cy} and H, are the cylinder diameter and the bed height, respectively.

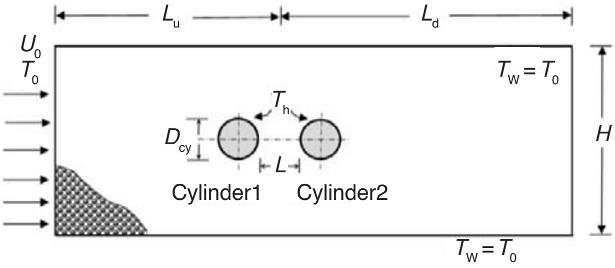

Figure 1. Schematic of the two tandem cylinder embedded in packed bed

The blockage ratio of the bed is small enough to neglect the channeling effect. It is supposed that the porous medium is homogenous and isotropic. There is no heat generation in the porous medium. Also, the radiation is neglected and local thermal equilibrium between the two phases is regarded.

Mathematical formulation

The 2-D governing equations are average-volume continuity, Darcy-Forchheimer momentum and local thermodynamic equilibrium (LTE) energy equation which are presented in vectorial form as the following [6, 17, 18 and 23]:

$$\nabla\langle\vec{\mathbf{u}}'\rangle = 0 \tag{1}$$

$$\frac{\rho_f}{\varepsilon}\left[\frac{\partial\langle\vec{\mathbf{u}}'\rangle}{\partial t'} + \frac{1}{\varepsilon}\langle(\vec{\mathbf{u}}'\nabla)\vec{\mathbf{u}}'\rangle\right] = -\frac{\mu_f}{K}\langle\vec{\mathbf{u}}'\rangle - \frac{\rho_f F\varepsilon}{\sqrt{K}}\left|\langle\vec{\mathbf{u}}'\rangle\right|\langle\vec{\mathbf{u}}'\rangle + \frac{\mu_f}{\varepsilon}\nabla^2\langle\vec{\mathbf{u}}'\rangle - \nabla\langle P_f'\rangle \tag{2}$$

$$(\rho C_p)_m\frac{\partial\langle T'\rangle}{\partial t'} + \varepsilon(\rho C_p)_f\left[\langle\vec{\mathbf{u}}'\rangle\nabla\langle T'\rangle\right] = \nabla\left[K_{eff}\nabla\langle T'\rangle\right] \tag{3}$$

The operator $\langle...\rangle$ used for the local average of a quantity and for velocity is calculated by:

$$\langle\vec{\mathbf{u}}'\rangle = \sqrt{u'^2 + v'^2} \tag{4}$$

Due to interaction of solid and fluid the mean energy capacity is used in eq. (3) that can be calculated by:

$$(\rho C_p)_m = \varepsilon(\rho C_p)_f + (1-\varepsilon)(\rho C_p)_s \tag{5}$$

Using the following dimensionless variables, transform the previous equations into dimensionless form:

$$x, y = \frac{x', y'}{D_{cy}}, \quad \vec{\mathbf{u}}' = \frac{\vec{\mathbf{u}}'}{u}, \quad \theta = \frac{T' - T_0}{T_h - T_0}, \quad P_f = \frac{P_f'}{\rho_f u_0^2} \tag{6}$$

So the eqs. (1)-(3) change to the following relations:

$$\nabla\langle\vec{\mathbf{u}}'\rangle = 0 \tag{7}$$

$$\frac{\partial\langle\vec{\mathbf{u}}\rangle}{\partial t} + \frac{1}{\varepsilon}\langle(\vec{\mathbf{u}}\nabla)\vec{\mathbf{u}}\rangle = -\frac{\varepsilon}{\mathrm{Re_D\,D_a}}\langle\vec{\mathbf{u}}\rangle + -\frac{F\varepsilon^2}{\sqrt{\mathrm{D_a}}}\left|\langle\vec{\mathbf{u}}\rangle\right|\langle\vec{\mathbf{u}}\rangle + \frac{1}{\mathrm{Re_D}}\nabla^2\langle\vec{\mathbf{u}}\rangle - \varepsilon\nabla\langle P_f\rangle \tag{8}$$

$$\frac{\partial\langle\theta\rangle}{\partial t}+\frac{\varepsilon}{C}\Big[\langle\vec{\mathbf{u}}\rangle\nabla\langle\theta\rangle\Big]=\frac{1}{\mathrm{Re_D}\,\mathrm{Pr}\,C}\nabla\left[\frac{K_{\mathrm{f.eff}}}{k_{\mathrm{f}}}\nabla\langle\theta\rangle\right] \tag{9}$$

where $C = \varepsilon + (1 - \varepsilon)(k_r / \alpha_r)$ and k_r and α_r are the solid/fluid thermal conductivity and diffusivity ratios, $k_\mathrm{s} / k_\mathrm{f}$ and $\alpha_\mathrm{s} / \alpha_\mathrm{f}$, respectively. The Reynolds, Darcy, Prandtl, and Biot numbers are defined, respectively:

$$\mathrm{Re_D}=\frac{u_0 D_{\mathrm{cy}}\rho_{\mathrm{f}}}{\mu_{\mathrm{f}}},\ \mathrm{Da}=\frac{K}{D_{\mathrm{cy}}^2},\ \mathrm{Pr}=\frac{\nu_{\mathrm{f}}}{\alpha_{\mathrm{f}}},\ \text{and Bi}=\frac{D_{\mathrm{cy}}^2 h_{\mathrm{sf}} a_{\mathrm{sf}}}{k_{\mathrm{s}}} \tag{10}$$

Duallien [24], suggested the following relation for the specific surface area:

$$a_{sf}=\frac{6(1-\varepsilon)}{d_p} \tag{11}$$

Wakao *et al*. [25], introduced the interfacial heat transfer coefficient:

$$h_{sf}=\frac{k_{\mathrm{f}}}{d}\left[2+\mathrm{Pr}^{1/3}\left(\frac{\rho_{\mathrm{f}}|\vec{\mathbf{u}}|d_p}{\mu_{\mathrm{f}}}\right)^{0.6}\right] \tag{12}$$

Ergun [26] suggested relations for the permeability and geometric function:

$$K=\frac{\varepsilon^3 d_p^2}{150(1-\varepsilon)^2},\quad F=\frac{1.75}{\sqrt{150\varepsilon^3}} \tag{13}$$

and the effective thermal conductivity is defined as $k_{\mathrm{f,eff},(x,y)} = k_{st} + k_{d(x,y)}$ [27], offered the semi-theoretical model for stagnant conductivity:

$$\frac{k_{st}}{k_{\mathrm{f}}}=\left(1-\sqrt{1-\varepsilon}\right)+\frac{2\sqrt{1-\varepsilon}}{1-\lambda B}\left[\frac{(1-\lambda)B}{(1-\lambda B)^2}\ln(\lambda B)-\frac{B+1}{2}-\frac{B-1}{1-\lambda B}\right]$$
$$\lambda=\frac{1}{K_r},\qquad B=1.25\left(\frac{1-\varepsilon}{\varepsilon}\right)^{10/9} \tag{14}$$

Wakao and Kaguei [28], based on experimental correlations in longitudinal and lateral directions define the dispersion conductivity which is the result of tortuous path around particles:

$$\frac{k_{dx}}{k_{\mathrm{f}}}=0.5\,\mathrm{Pr}\left(\frac{\rho_{\mathrm{f}}|\mathbf{u}|d_p}{\mu_{\mathrm{f}}}\right),\ \frac{k_{dy}}{k_{\mathrm{f}}}=0.1\,\mathrm{Pr}\left(\frac{\rho_{\mathrm{f}}|\mathbf{u}|d_p}{\mu_{\mathrm{f}}}\right) \tag{15}$$

and the solid effective thermal conductivity is $k_{\mathrm{s,eff}} = (1- \varepsilon)\, k_\mathrm{s}$. It is assumed that the fluid and solid phases share the same temperature as the isothermal surface of the cylinder. In other words, thermal equilibrium is imposed at the heated boundary. To evaluate the heat transfer the time-mean average Nusselt number along the heated cylinder for solid and fluid phases is used with the following relation:

$$\mathrm{Nu_f}=\frac{h_{\mathrm{cy}}D_{\mathrm{cy}}}{k_{\mathrm{f}}},\ \mathrm{Nu_s}=\frac{h_{\mathrm{cy}}D_{\mathrm{cy}}}{k_{\mathrm{s}}} \tag{16}$$

The viscous resistance in a packed bed is equal to [29]:

$$R_v = \frac{150(1-\varepsilon)^2}{\phi^2 {d_p}^2 \varepsilon^3} \tag{17}$$

that d_p is the diameter of particles in packed bed and ϕ is sphericity of particles. The inertial resistance is calculated with [29]:

$$R_i = \frac{2\times 1.75\times(1-\varepsilon)}{\phi d_p \varepsilon^3}, \quad \phi = \left(\frac{6}{d_p}\right)\left(\frac{S_\mathrm{p}}{V_\mathrm{p}}\right) \tag{18}$$

S_p and V_p are the surface area and the volume of the particle, respectively. For spherical particles sphericity is equal to 1.0. So the total pressure drop is equal to:

$$\frac{\mathrm{d}_p}{\mathrm{d}_l} = \mathrm{Re}\,\mu u + \left(\frac{R_i}{2}\right)\rho u^2 \tag{19}$$

Numerical solution

The computational domains are made based on the results of [16, 17]. The governing equations are numerically solved using the finite volume method. The convection and diffusion fluxes on the faces of control volume are interpolated with high order upwind and central differences. Figure 3 indicated the computational domain which is made with triangular grids as fig. 2 and finer grid near solid walls was generated. The independency of results to grid resolution, at different grids are examined for $D_\mathrm{cy}/d_p = 10$, $\varepsilon = 0.37$. The variation of mean fluid Nusselt number, which is chosen as a control parameter, *vs.* different grid number is shown in fig. 3. It seems that if the domain includes at least $2\cdot 10^4$ nodes, the grid impendency is obtained and the difference between the results less than 0.1%.

For validation of the present numerical method, first the problem of two tandem cylinder, is solved and in fig. 4 present streamlines are compered of the experimental results of [15, 16, 19]. Second, the problem of flow over a cylinder, which is embedded in a porous medium, is considered. Figure 5 shows the variation of mean fluid Nusselt number *vs.* different Peclet number around one cylinder embedded in a packed bed of aluminum particles and compared with the results of previous works [30, 31]. It is observed that the results of experimental, analytical, and present numerical work are in a good accordance.

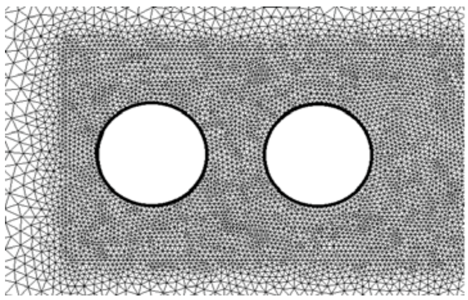

Figure 2. Generated mesh, using finer meshes near and behind the cylinders

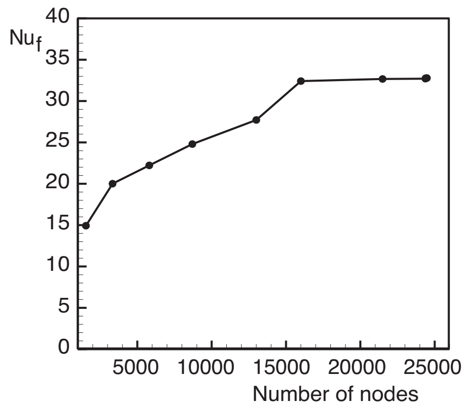

Figure 3. Mean fluid Nusselt number around cylinder 1 *vs.* number of nodes, in porous channel with Pr = 5.49, Pe = 150

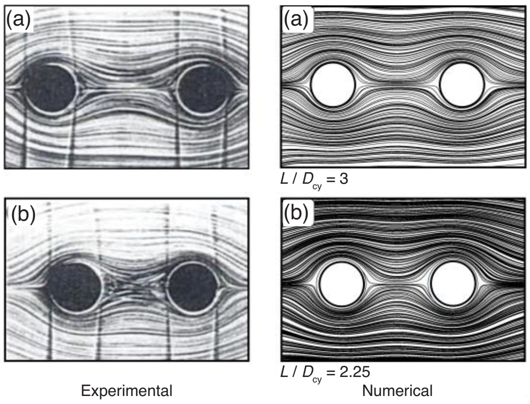

Figure 4. Flow past two tandem cylinders at Re = 0.02; comparison the results of numerical present work and the experimental results [15, 16, 19]

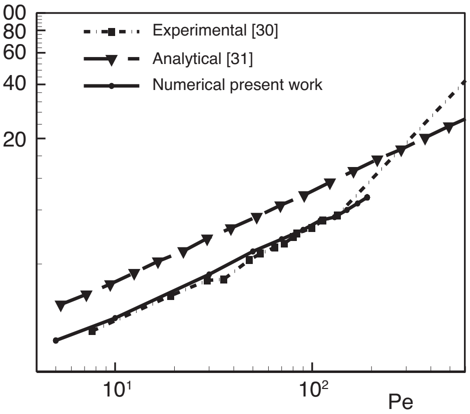

Figure 5. Mean fluid Nusselt number *vs.* Peclet number for a cylinder embedded in porous channel D_{cy} = 0.012, Pr = 5.49

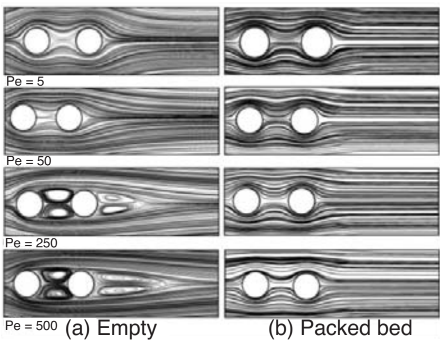

Figure 6. Flow streamlines in empty and porous channel *vs.* Peclet number at L/D_{yc}, Pr = 5.49

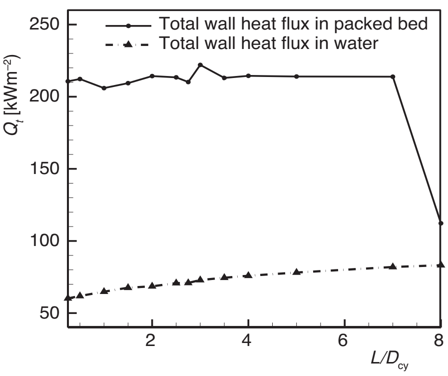

Figure 7. Comparison of total wall heat flux in empty and porous channel *vs.* horizontal distances between two cylinders, Pr = 5.49, Pe = 150

Results and discussion

Figure 6 compares the flow streamlines around two tandem cylinders in L/D_{cy} = 1 with Pr = 5.49 in different velocities. In the column (a) by increase the velocity, due to separation a wake region is seen and growth by increment in velocity so that it can cover two cylinders and a closed vortex region may generated. But in the column (b), the channel filled with solid aluminum particles. Due to interaction of fluid and solid particles, the flow velocity can not increase, therefore the separation does not happen. So the flow pattern in porous has no significant changes in different velocities and there is no closed vortex region here. All the comparisons in the following figures are performed in very low Reynolds numbers and in long distances between two cylinders, so that the two cylinders are not located in closed vortex region in empty channels. Figure 7 compares the total wall heat flux of two cylinders in pure water and water passes through packed bed of aluminum particles and when the water passes through the packed bed the heat transfer increase, considerably. The maximum heat from cylinders in porous is Q_{max} = 222.05 kW/m^2 and in empty channel is Q_{max} = 74.54 kW/m^2. So by using porous channel the heat transfer about three times increased and this is the main reason of using the porous channels, especially in compact nuclear heat exchangers in which the limitations of distances and time are too important. In the packed bed, the total wall heat flux has a significant increment with increasing the distance of two cylinders up to $L/D_{\mathrm{cy}} = 3$ and after this distance the trend of wall heat flux changes.

In fig. 8 the fluid mean Nusselt number *vs*. horizontal distance between the two cylinder is drawn and it is obvious that in $L/D_{\mathrm{cy}} = 3$ there is a local maximum. But in the empty channel, the total wall heat flux has a mild increment with increasing the distance of two cylinders. Another effect of using packed bed is the change in the pressure contours and pressure gradient.

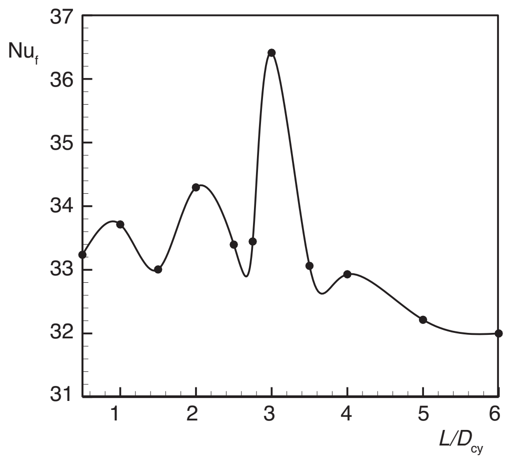

Figure 8. Mean fluid Nusselt number in packed bed *vs.* the horizontal distance of two cylinders, Pr = 5.49, Pe = 150

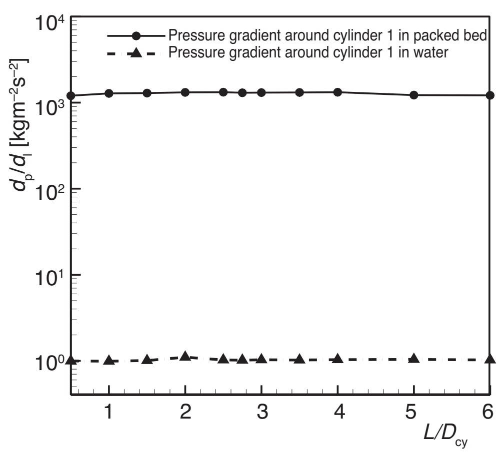

Figure 9. Comparison of the pressure gradient around cylinder 1 in empty and porous channel, *vs.* the horizontal distance of two cylinders, Pr = 5.49, Pe = 150

Figure 9 compares the pressure gradient around cylinder 1, in empty and porous channels. As it is expected, with increase the solid particles, the interaction between the solid and fluid molecules causes significant pressure drop in fluid flow.

Figure 10 compares the pressure contour lines in empty and porous channels. Due to increase the porous particles, the pressure contours around two cylinder changes to uniform state, especially in the distance between two cylinders the difference between empty and porous channel is notable. Figure 11 indicates the fluid non-dimensional outlet temperature in water and cylinders embedded in porous medium. The fluid outlet temperature in porous medium is greater than water.

Figure 12 shows the variation of the fluid and solid mean Nusselt number around cylinder 1 when the water passing through the porous channel. The solid

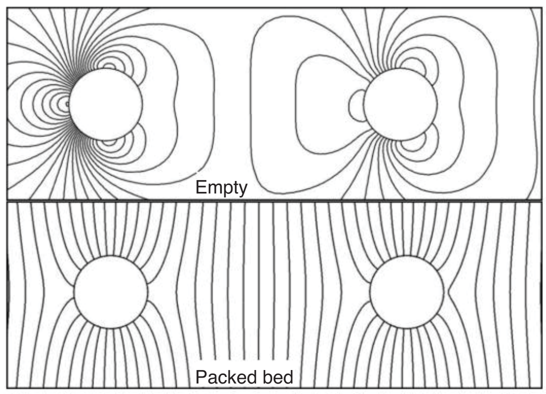

Figure 10. Comparison of the Pressure Contours in empty and porous channel at $L/D_{cy} = 3$ and Pr = 5.49, Pe = 150

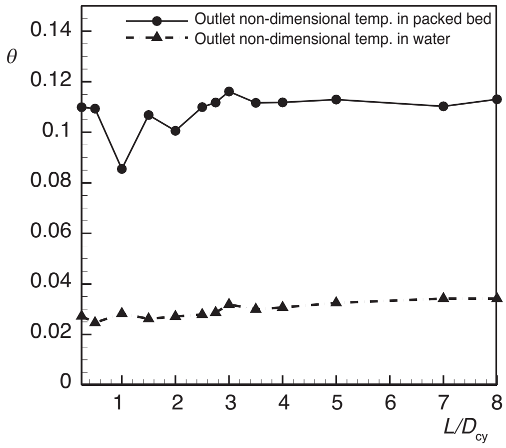

Figure 11. Comparison of the fluid non-dimensional outlet temperature *vs.* the horizontal distance of two cylinders, Pr = 5.49, Pe = 150

particles absorb a part of heat form the cylinder. The share of fluid particles is greater than the solid particles. The physical explanation of the difference between empty and porous channels is presented. First it should be noted that in porous medium solid particles change the streamlines, pressure gradient and pressure contours to a more uniform state, so the regime of the fluid changes extremely. There is no wake between the two cylinders and behind the second cylinders. While the flow uniformly and slowly passes the channel, it better absorb the heat from the wall cylinders and solid particles. Second, due to interaction between solid particles and two cylinder walls, they absorb the heat from the cylinders because aluminum has very high thermal conductivity coefficient. Third, due to the interaction of fluid and solid particles in the packed bed, the absorbed heat from the solid particles easily transfer to fluid particles. Now, if the air passes the channel with the same geometry and porous materials, the same trends are seen. Figure 13 compares the total wall heat fluxes of two tandem circular cylinders in empty and porous channel with Pr = 0.715. The same as water, it is seen that for the porous medium, the maximum heat transfer is obtained at $L/D_{cy} = 3$. The comparison of figs. 7 and 13 shows that, the quantities of max heat fluxes for the air are lower than water because air has lower heat capacity, density and Prandtl number. That means increase the Prandtl number of fluid in the packed bed resulted in an increase in the total heat fluxes, significantly.

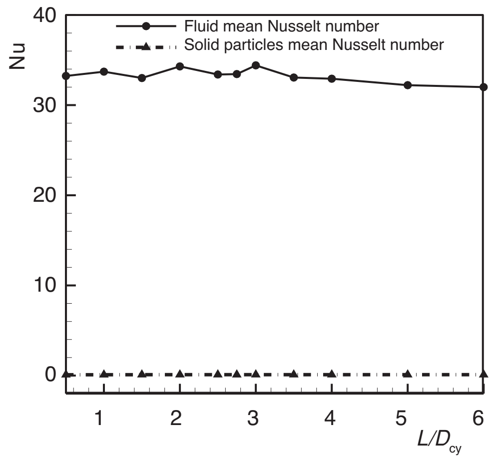

Figure 12. Mean Nusselt number of the fluid and solid particles in packed bed *vs.* the horizontal distance of two cylinders, Pr = 5.49, Pe = 150

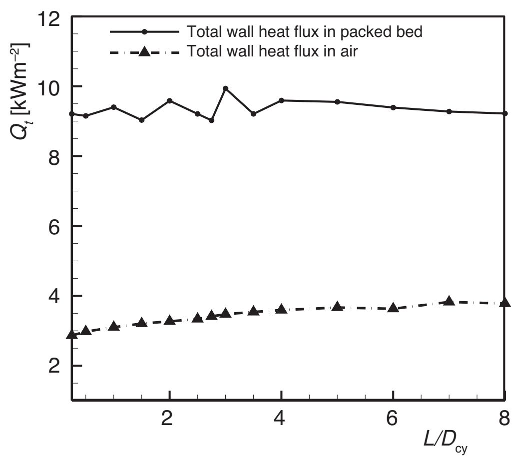

Figure 13. Total wall heat flux in empty and porous channel *vs.* the horizontal distance of two cylinders Pr = 0.715, Pe = 150

Figure 14, clearly shows the total wall heat flux in porous channel has a local maximum at $L/D_{cy} = 3$. When the laminar flow reaches to first cylinder, fluid particles absorbs amount of heat from cylinder. After passing the first cylinder, in the distance between two cylinders, the interaction of fluid-solid particles causes a heat transfer and reduction in temperature. *Vice versa*, increase the distance causes the loss in heat transfer because of the growth of the pressure drop and reduction of the velocity. So, it should be an optimum point for this distance and as fig. 14 shows, it takes place in $L/D_{cy} = 3$. It can be an applicable matter in packed bed piping. But in empty channel the trend of the total heat transfer is different. It is seen that in empty channel there is a mild increment in total heat transfer with increasing the distance between the cylinders.

Figure 15 comparison of the streamlines in empty channel *vs*. the horizontal distance of two cylinders, $\mathrm{Pr} = 0.715$, $\mathrm{Pe} = 150$. It shows the streamlines of air in empty *vs*. the variation of horizontal distance between two cylinders. Here, with increase the distances between two cylinder the wake after the cylinder 1 is diminishes and the streamlines of flow behind the cylinder 1 attached to each other and the wakes behind it disappears, so the flow can absorb the second cylinder wall heat fluxes easily and therefore the overall heat flux and outlet temperature increases and especially the total wall heat flux has a continuous increment with increasing the horizontal distance, although its quantity is more lower than which belong to porous channel.

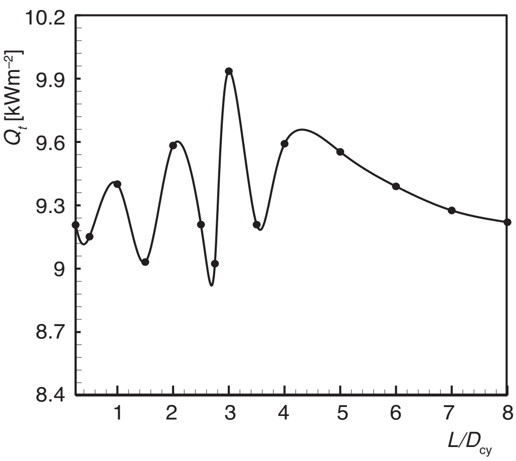

Figure 14. Total wall heat flux in porous channel *vs*. the horizontal distance of two cylinders, Pr = 0.715, Pe = 150

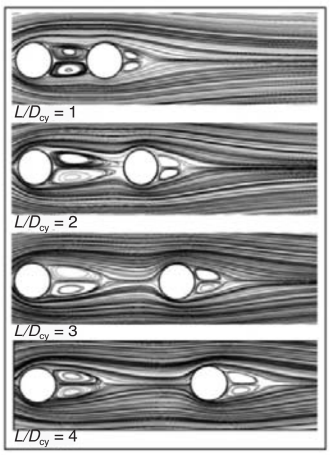

Figure 15. Comparison of the stream lines in empty channel *vs*. the horizontal distance of two cylinders, Pr = 0.715, Pe = 150

Figure 16 shows the pressure gradients around the first and second cylinders are different, significantly. The pressure gradient around the first cylinder is much higher than the pressure gradient around the second cylinder. The pressure gradient around the second cylinder increased with increase the distance of two cylinders. Figure 17 shows the difference between the pressure gradient in pure air and packed bed around cylinder 1. The quantities for air are lower than the pressure gradients for the water.

Figure 18 indicates the non-dimensional outlet temperature in empty and porous medium. The outlet temperature in packed bed is greater than empty channel considerably. Also, the air outlet temperature is lower than the water outlet temperature in both empty air and air passes through packed bed. Figure 19 shows the contour lines of temperature for air passing the porous channel contains the two embedded tandem cylinders *vs*. the distance between the cylinders. With increase the horizontal distance between cylinders, the isotherm lines between two cylinders becomes uniform. The physical explanation which presented for the empty and porous channel when the air is the working fluid is the same as what presented previously for the water.

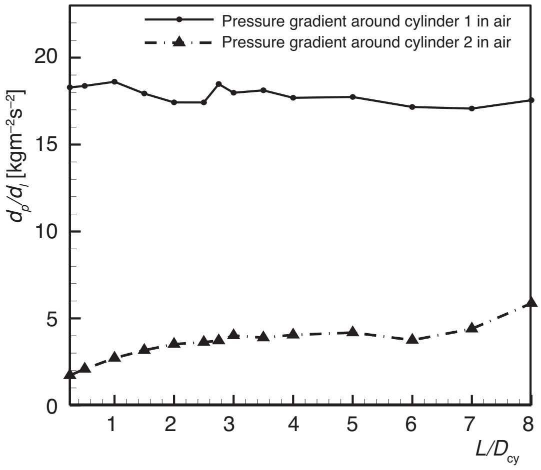

Figure 16. Pressure gradient around two tandem cylinder in empty channel *vs.* the horizontal distance of two cylinders, Pr = 0.715, Pe = 150

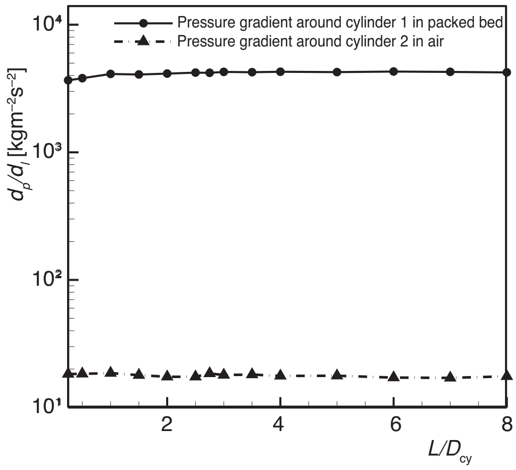

Figure 17. Comparison of the pressure gradient around cylinder 1 in empty and porous channel *vs.* the horizontal distance of two cylinders, Pr = 0.715, Pe = 150

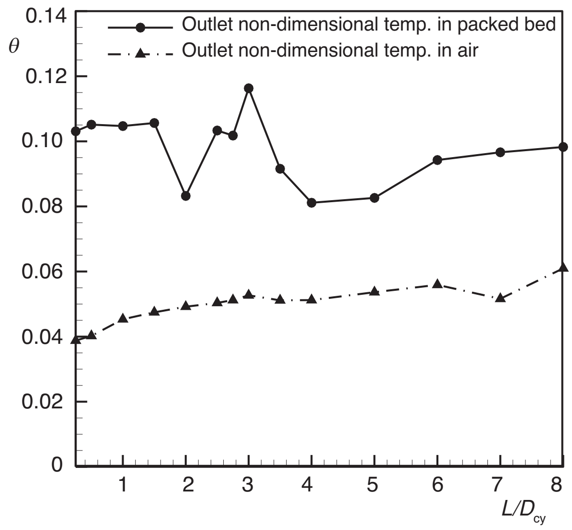

Figure 18. Comparison of the fluid non-dimensional outlet temperature in empty and porous channel vs. the horizontal distance of two cylinders, Pr = 0.715, Pe = 150

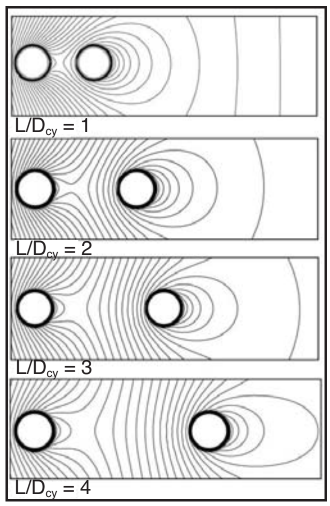

Figure 19. Temperature contours in porous channel *vs.* the horizontal distance of two cylinders, Pr = 0.715, Pe = 150

Conclusions

In the present work, forced convection heat transfer from two tandem circular cylinders embedded in a porous medium is investigated. The porous channel included the aluminum spherical particles and it is shown the presence of porous medium, enhances the overall heat transfer. At the same time, change the pressure contours and increases the pressure drop in the channel significantly. Comparison of the pressure gradients in empty and porous channels indicates that the length of the porous channel should be as much as shorter due to high pressure gradient. The horizontal distance between two tandem cylinders is a main factor that changes the total wall heat fluxes from two tandem cylinders in porous medium and at the distance about three times of cylinder diameter in laminar flow, the maximum of heat absorption from two cylinders is obtained. Increasing the distance more than this quantity, causes reduction in overall wall heat flux. The outlet temperature of the fluid in porous channel is greater that the empty channel. In empty channel there is a very low increase in heat transfer absorbed from two cylinders with increment the distance.

Nomenclature

a_{sf} – specific interfacial area, [m^{-1}]
C_p – specific heat capacity, [Jkg^{-1}K^{-1}]
d_p – particle diameter, [m]
D_{cy} – cylinder diameter, [m]
Da – Darcy number, (= k/D_{cy}^2)
F – geometric function
h_{sf} – interfacial heat transfer coefficient, [Wm^{-2}K^{-1}]
H – channel height, [m]
K – permeability, [= $\varepsilon^3 d^2_p/150(1-\varepsilon)^2$], [m^2]
k – thermal conductivity, [Wm^{-1}K^{-1}]
k_r – solid/fluid thermal conductivity ratio, $k_r = k_s/k_f$
L – horizontal distance between two cylinder, [m]
Nu – time mean average Nusselt number
P_f' – fluid pressure, [Nm^{-2}]
P_f – dimensionless fluid pressure
Pr – Prandtl number, (= ν_f/α_f)
Q_t – total wall heat flux, [Wm^{-2}]
$\mathrm{Re_D}$ – Reynolds number, (= $u_0\rho_f D_{cy}/\mu_f$)
R_i – inertial resistance
R_v – viscous resistance
t' – time, [s]
t – dimensionless time
T' – temperature, [K]
T_h – cylinder wall temperature, [K]
$\vec{\mathbf{u}}'$ – vectorial fluid velocity, [ms^{-1}]
$\vec{\mathbf{u}}$ – dimensionless vectorial velocity, (= $\mathbf{u}/u_0$)
u' – horizontal velocity component, [ms^{-1}]
u – dimensionless horizontal velocity component
u_0 – inlet horizontal fluid velocity, [ms^{-1}]
v' – vertical velocity component, [ms^{-1}]
v – dimensionless vertical velocity component
x', y' – horizontal and vertical co-ordinates, [m]
x, y – dimensionless horizontal and vertical coordinates

Greek symbols

α – thermal diffusivity, [m^{2}s^{-1}]
α_r – solid-to-fluid thermal diffusivity ratio, (= α_s/α_f)
ε – porosity
θ – dimensionless temperature, [= $(T - T_0)/(T_h - T_0)$]
μ_f – fluid dynamic viscosity, [kgm^{-1}s^{-1}]
ρ_f – fluid density, [kgm^{-3}]
ϕ – sphericity of particles

Subscripts

eff – efective
f – fluid
s – solid

References

[1] Goldstein, R. J., *et al*., Heat Transfer – A Review of 2004 Literature, *Int. J. of Heat and Mass Transfer, 53*, (2010), 21-22, pp. 4343-4396
[2] Vafai, K., *Porous Media-Application in Biological Systems and Biotechnology*, Taylor and Francis, Oxford, UK, 2011
[3] Kwapinski, W., *et. al*., Modeling of the Wall Effect in Packed Bed Adsorption, *Chemical Engineering and Technology, 27* (2004), 11, pp. 1179-1186
[4] Thomeo, J. C., Grace, J. R., Heat Transfer in Packed Beds: Experimental Evaluation of One-Phase Water Flow, *Brazilian J. of Chemical Engineering*, *21* (2004), 1, pp. 13-22
[5] Teplitskii, Y. S., Heat Exchange in a Tube Flled with Granular Bed, *J. of Engineering Physics and Thermophysics, 77* (2004), 1, pp. 103-110
[6] Kaviany, M., *Principles of Heat Transfer in Porous Media*, 2nd ed., Springer, New York, USA, 1998
[7] Mahgoub, S. E., Forced Convection Heat Transfer Over a Flat Plate in a Porous Medium, *Ain Shams Engineering Journal, 4*, (2013), 4, pp. 605-613
[8] Hellstrom, J. G. I., Lundstrom, T. S., Flow through Porous Media at Moderate Reynolds Number, *Proceedings*, Int. Scientific Colloquium Modeling for Material Processing, Riga, 2006

[9] Vafai, K., *Handbook of Porous Media*, 2ed ed., Taylor and Francis, New York, USA, 2005
[10] Yuki, K., *et al*., Flow Visualization and Heat Transfer Characteristics for Sphere-Packed Pipes, *J. of Thermophysics and Heat Transfer, 22* (2008), 4, pp. 632-648
[11] Orodu, O. D., *et al*., Experimental Study of Darcy and Non-Darcy Flow in Porous Media, *Int. J. of Engineering and Technology*, *2* (2012), 2, pp. 1934-1943
[12] Verma, N., Mewes, D., Lattice Boltzmann Methods for Simulation of Micro and Macro-Transport in a Packed Bed of Porous Adsorbents under Non-Isothermal Condition, *Computers and Mathematics with Applications, 58* (2009), 5, pp. 1003-1014
[13] Peng, Y.-F., *et al*., Nested Cartesian Grid Method in Incompressible Viscous Fluid Flow, *J. of Computational Physics, 229* (2010), 19, pp. 7072-7101
[14] Zdravkovich, M. M., *Flow around Circular Cylinders*, Vol. 1: *Fundamentals*, Oxford Science Publications, Oxford, UK, 1997
[15] Zdravkovich, M. M., *Flow around Circular Cylinders*, Vol. 2: *Applications*, Oxford Science Publications, Oxford, UK, 2002
[16] Tatsuno, M., *et al*., On the Stable Posture of a Triangular or a Square Cylinder about Its Central Axis in a Uniform Flow., *Fluid Dyn. Res*., *6* (1990), 3-4, pp. 201-207
[17] Al-Sumaily, G. F., *et al*., Analysis of Forced Convection Heat Transfer from a Circular Cylinder Embedded in a Porous Medium, *Int. J. of Thermal Sciences, 51* (2012), Jan., pp. 121-131
[18] Al-Sumaily, G. F., *et al*., The Effect of Porous Media Particle Size on Forced Convection from a Circular Cylinder without Assuming Local Thermal Equilibrium between Phases, *Int. J. of Heat and Mass Transfer, 55* (2012), 13-14, pp. 3366-3378
[19] Kostic, Z. G., Oka, S. N., Fluid Flow and Heat Transfer with Two Cylinders in Cross Flow, *J. of Heat and Mass Transfer, 15* (1972), 2, pp. 279-299
[20] Dehkordi, B. G., *et al.*, Numerical Simulation of Flow over Two Circular Cylinders in Tandem Arrangement, *J. of Hydrodynamics, 23* (2011), 1, pp. 114-126
[21] Koda, Y., Lien, F.-S., Aerodynamic Effects of the Early Three-Dimensional Instabilities in the Flow over One and Two Circular Cylinders in Tandem Predicted by the Lattice Boltzmann Method, *Computers & Fluids, 74* (2013), Mar., pp. 32-43
[22] Shyam, R., Chhabra, R. P., Effect of Prandtl Number on Heat Transfer from Tandem Square Cylinders Immersed in Power-Law Fluids in the Low Reynolds Number Regime, *International Journal of Heat and Mass Transfer, 57* (2013), 2, pp. 742-755
[23] Nield, D. A., Bejan, A., Convection in Porous Media, 3rd ed., Springer Science, Business Media, New York, USA, 2006
[24] Dullien, F. A., *Media Fluid Transport and Pore Structure*, Academic Press, New York, USA, 1979
[25] Wakao, N., *et al*., Effect of Fluid Dispersion Coefficients on Particle-to-Fluid Heat Transfer Coefficients in Packed Beds-Correlation of Nusselt Numbers, *Chem. Eng. Sci*., *34* (1979), 3, pp. 325-336
[26] Ergun, S., Fluid Flow through Packed Columns, *Chem. Eng. Prog. 48* (1952), 2, pp. 89-94
[27] Zehner, P., Schluender, E. U., Thermal Conductivity of Granular Materials at Moderate Temperatures, *Chem. Ing. Tech*., *42* (1970), 14, pp. 933-941
[28] Wakao, N., Kaguei, S., *Heat and Mass Transfer in Packed Beds,* Gordon and Breach, Philadelphia, Penn., USA, 1982
[29] ***, ANSYS Fluent Tutorial Guide, Release 15.0, (10), 2013, pp. 445-480
[30] Nasr, K., *et al*., Experimental Investigation on Forced Convection Heat Transfer from a Cylinder Embedded in a Packed Bed, *J. Heat Transfer 116* (1994), 1, pp. 73-80
[31] Cheng, P., Mixed Convection about a Horizontal Cylinder and a Sphere in a Fluid Saturated Porous Medium, *Int. J. Heat Mass Transfer 25*, (1982), 8, pp. 1245-1247

Paper submitted: March 7, 2015
Paper revised: April 20, 2015
Paper accepted: May 19, 2015